Rhodopseudomonas palustris CGA009 Has Two Functional *ppsR* Genes, Each of Which Encodes a Repressor of Photosynthesis Gene Expression†

Stephan Braatsch,‡ Jeffrey R. Bernstein,§ Faith Lessner,|| Jennifer Morgan,|| James C. Liao,§ Caroline S. Harwood,⊥ and J. Thomas Beatty*,‡

Department of Microbiology and Immunology, University of British Columbia, 2350 Health Sciences Mall, Vancouver, British Columbia V6T 1Z3, Canada, Department of Chemical Engineering, University of California, 5531 Boelter Hall, 420 Westwood Plaza, Los Angeles, California 90095, Department of Microbiology, University of Iowa, Iowa City, Iowa 52242, and Department of Microbiology, University of Washington, Box 357242, Seattle, Washington 98195-7242

Received May 30, 2006; Revised Manuscript Received August 17, 2006

ABSTRACT: The PpsR protein is a regulator of redox-dependent photosystem development in purple phototrophic bacteria. In contrast to most species, *Rhodopseudomonas palustris* contains two *ppsR* genes. We show that the inactivation of each of the *R. palustris* strain CGA009 *ppsR* genes results in an elevated level of formation of the photosystem under dark aerobic conditions. Absorption spectra of the two PpsR mutants revealed qualitative and quantitative differences in light-harvesting peak amplitude increases. A sequence difference in the helix−turn−helix DNA binding motif of PpsR2 (Arg 439 to Cys) between *R. palustris* strains CEA001 and CGA009 is shown to be a natural polymorphism that does not inactivate the repressor activity of the protein. To evaluate which photosynthesis genes are regulated by the two PpsR proteins, transcriptome profiles of the CGA009 and PpsR mutant strains were analyzed in microarray experiments. Transcription of most but not all photosystem genes was derepressed in the mutant strains to levels consistent with the in vivo absorption spectra, mathematical analyses of peak shapes and amplitudes, reaction center protein levels, and real-time PCR of selected mRNAs. Closely spaced PpsR binding motif repeats were identified 5′ of genes that were derepressed in the transcriptome analysis of PpsR mutants. This work shows that both the PpsR1 and PpsR2 proteins from *R. palustris* strain CGA009 function as oxygen-responsive transcriptional repressors.

Purple non-sulfur phototrophic bacteria such as *Rhodopseudomonas palustris* are capable of aerobic growth using oxidative phosphorylation, or of anaerobic phototrophic growth using photophosphorylation (*1*). The development of a membrane-bound photosynthetic apparatus is stimulated by O_2 deprivation. This O_2-regulated photosystem includes the photosynthetic reaction center (RC)[1] and light-harvesting complexes, which bind bacteriochlorophyll (BChl) and carotenoid (Crt) pigments to capture light energy (*2*). *R. palustris* has three kinds of light-harvesting (LH) complexes designated LH1, LH2, and LH4, with LH2 variants encoded by three operons (*1*, *3*). Several regulatory systems (*2*), including PpsR (called CrtJ in *Rhodobacter capsulatus*), a DNA-binding protein unique to purple phototrophic bacteria, modulate transcription of photosynthesis genes in response to the O_2-dependent redox state of cells (*4*).

The function of PpsR proteins has been studied in several species that encode PpsR orthologues that are 29−55% identical in amino acid sequence (*5*−*14*). All PpsR proteins contain *Per*−*Arnt*−*Sim* (PAS) and helix−turn−helix (HTH) motifs (Figure 1A), and it seems that a key element of redox-dependent PpsR activity is the presence of one or more cysteine residues, either for intraprotein disulfide bond formation as in *Rhodobacter* species (*6*, *7*) or for interprotein disulfide bonding as in the PpsR1 of *Bradyrhizobium* ORS278 (*11*, *14*). Although most PpsR proteins repress transcription of photosynthesis genes in response to high (positive) redox conditions, there are significant species-specific differences. For example, the redox-dependent repressor activity of *Rhodobacter sphaeroides* PpsR, but not the highly similar *Rh. capsulatus* CrtJ, is antagonized by blue light illumination (*15*). This light regulation results from a direct interaction of the *Rh. sphaeroides* PpsR with the light-sensing AppA protein (*7*), which is absent from *Rh. capsulatus*. Additionally, the PpsR of *Rubrivivax gelatinosus* was reported to act as both a high-redox repressor and a low-redox activator of different photosynthesis genes (*5*), and PpsR1 of *Bradyrhizobium* ORS278 appears to activate gene expression (*11*).

†This research was supported by the Office of Science (BER), U.S. Department of Energy Grant DE-FG02-01ER63241 (J.C.L., C.S.H., and J.T.B.), The Boehringer Ingelheim Fonds, Travel Allowances (S.B.), and the Division of Energy Biosciences, U.S. Department of Energy (Grant DE-FG02-05ER15707 to C.S.H.).

* To whom correspondence should be addressed. Phone: (604) 822-6896. Fax: (604) 822-6041. E-mail: jbeatty@interchange.ubc.ca.

‡ University of British Columbia.

§ University of California.

|| University of Iowa.

⊥ University of Washington.

[1] Abbreviations: Bchl, bacteriochlorophyll; Crt, carotenoid; HTH, helix−turn−helix; LH1, light-harvesting complex 1; LH2, light-harvesting complex 2; LH4, light-harvesting complex 4; PAS, *Per*−*Arnt*−*Sim*; PS, photosynthetic complex; RC, reaction center; RT-PCR, real-time polymerase chain reaction; SDS−PAGE, sodium dodecyl sulfate−polyacrylamide gel electrophoresis.

10.1021/bi061074b CCC: $33.50
Published on Web 11/08/2006

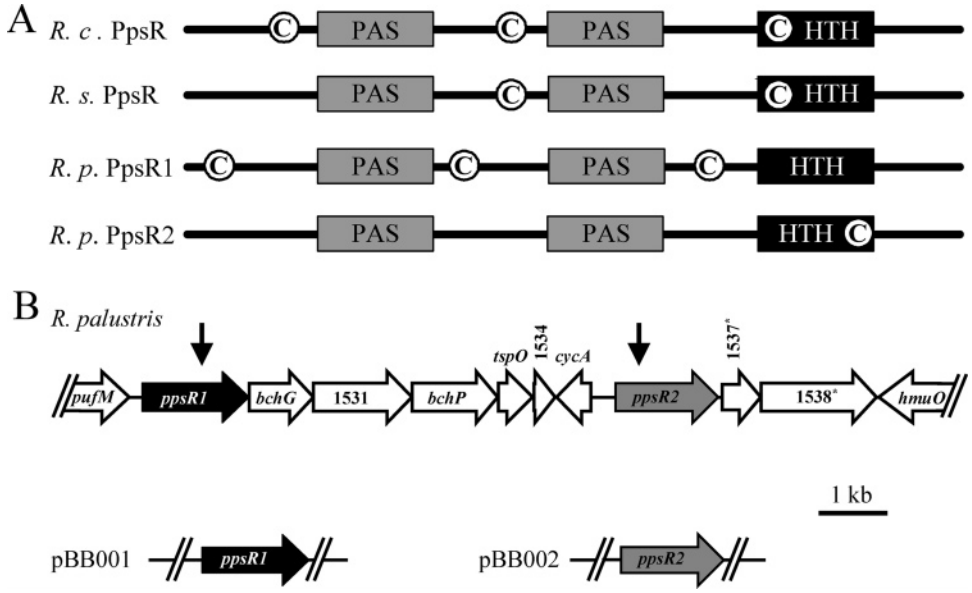

FIGURE 1: (A) Domain structure of PpsR proteins. Abbreviations: C, cysteine; HTH, helix−turn−helix motif; PAS (*Per−Arnt−Sim*), motif involved in sensory transduction by either binding small cofactors or protein−protein interactions (*44*); *R.c.*, *Rh. capsulatus*; *R.p.*, *R. palustris* CGA009; *R.s.*, *Rh. sphaeroides*. (B) Arrangement of the genes located around *ppsR1* and *ppsR2* in *R. palustris* CGA009. Horizontal arrows indicate the direction of transcription. Gene names or numbers (RPA#) from the annotated genome are given, and asterisk denotes the frameshifted *bphB* pseudogene in strain CGA009 (*1*, *14*). Vertical arrows represent the mini-Tn5 *lacZ*1 (*22*) insertion in the 3′−5′ direction (backward) into *ppsR1* (resulting in *R. palustris* PPSR1$^-$) or *ppsR2* (resulting in *R. palustris* PPSR2$^-$). pBB001 and pBB002 represent plasmids used to complement the single insertion mutations in PPSR1$^-$ and PPSR2$^-$, respectively.

The discovery of two *ppsR* gene orthologues in *R. palustris* and *Bradyrhizobium* ORS278, in similarly organized photosynthesis gene clusters (*1*, *18*), raised the question of whether both genes are functional and, if so, whether their gene products act as activators or repressors. In addition to the presence of two *ppsR* genes, *R. palustris* and *Bradyrhizobium* ORS278 differ from other purple bacteria in the presence of a bacteriophytochrome gene (*bphP*) adjacent to the *ppsR2* gene in the photosynthesis gene cluster (Figure 1B). The BphP protein appears to respond to ~700−800 nm (far-red) light to strengthen photosynthesis gene expression during aerobic growth (*18*). A model for distinct roles for the two PpsR proteins in sensing redox (PpsR1) and light (PpsR2) was proposed for *Bradyrhizobium*, and it was suggested that this model also applies to *R. palustris* (*11*, *14*), although this was not directly addressed experimentally. In this model, PpsR1 is an activator of photosynthesis gene expression in response to low-redox conditions, analogous to one function of the *Ru. gelatinosus* PpsR (*5*). The *Bradyrhizobium* and *R. palustris* PpsR2 proteins were proposed to repress expression of photosynthesis genes in the absence of far-red light, and it was suggested that far-red light activates BphP to relieve PpsR2-dependent repression of photosynthesis genes (*18*). However, there is no experimental evidence for a direct interaction between the PpsR2 and BphP proteins.

It was also proposed (*14*) that genome-sequenced *R. palustris* strain CGA009 is defective in the regulation of photosynthesis gene expression because it contains *bphP* (RPA1537/1538) and *ppsR2* (RPA1536) mutations, as a result of laboratory cultivation, so that neither gene is functional. The *bphP* sequence change appears to be a genuine frameshift mutation, consistent with the available data (*1*), and we found that transcomplementation of CGA009 with the *bphP* gene restored the far-red light response (unpublished). Giraud et al. (*14*) suggested that the strain CGA009 *ppsR2* gene must also have a mutation. The *R. palustris* CGA009 *ppsR2* gene sequence differs from strain CEA001 *ppsR2* by a single nucleotide, with a Cys codon present in the CGA009 *ppsR2* gene instead of an Arg codon, corresponding to residue 439 in the HTH region (Figure 1A).

We took advantage of the *bphP* (RPA1537/1538) frameshift mutation of *R. palustris* CGA009 (*1*) to study the functions of PpsR1 and PpsR2 in the absence of possible light regulation mediated by BphP. Mutants of *ppsR1* and *ppsR2* were constructed and studied via absorption spectroscopy, Western blot analysis, gene array, and real-time RT-PCR experiments.

The phenotype of the *ppsR1* mutant described in this paper indicates that PpsR1 is an O_2-responsive repressor, instead of an activator of photosynthesis gene expression as previously suggested (*14*). In addition, we show that the *R. palustris* CGA009 PpsR2 protein is also a functional O_2-responsive repressor. We present a modified model for the complex regulation of photosynthesis gene expression in *R. palustris* CGA009 by two distinct PpsR proteins.

MATERIALS AND METHODS

Bacterial Strains and Culture Conditions. The strains are listed in Table 1. *R. palustris* strains were grown in the PM defined medium (*19*) with 10 mM succinate as the carbon source and 100 μg/mL gentamicin or 100 μg/mL kanamycin where indicated. Aerobic and semiaerobic cultures of *R. palustris* were grown at 30 °C without illumination in Erlenmeyer flasks filled to 8 and 80% of nominal capacity, respectively, and shaken at 250 and 150 rpm, respectively. Photosynthetic cultures were grown anaerobically in completely filled screw-cap tubes (20 mL) inoculated from semiaerobic cultures. Photosynthetic cultures were incubated at 30 °C in an aquarium filled with water and illuminated

Table 1: Bacterial Strains, Plasmids, and Primers

	relevant features[a]	reference or source
R. palustris		
CGA009	wild type, *bphP*$^-$	*1, 19*
PPSR1$^-$	CGA009 *ppsR*1::miniTn-5, Km^r	this study
PPSR2$^-$	CGA009 *ppsR*2::miniTn-5, Km^r	this study
CEA001	wild type	*14*
355	wild type	*30*
HAA3	wild type	*29*
API	wild type	*28*
NCIMB8288	wild type	*28*
BIS3	wild type	*31*
DCP3	wild type	*32*
RCH500	wild type, isolated from Woods Hole	this study
BISA52	wild type	*29*
BISA14	wild type	*29*
E. coli		
DH5α	strain used for cloning	NEB
S17-I	Tra$^+$ strain used for plasmid mobilization	*43*
S17-I λpir	S17-I lysogenized with λpir phage	*22*
plasmid		
pUTminiTn-5 *lacZ*1	promoterless *lacZ*; Km^r	*22*
pBBR1MCS-5	broad-host-range cloning vector; Gm^r	*27*
pBB001	pBBR1-MCS5 based, carries *ppsR1* plus 262 bp upstream region; Gm^r	this study
pBB002	pBBR1-MCS5 based, carries *ppsR2* plus 322 bp upstream region; Gm^r	this study
primer		
*ppsR*1 F	5′-TAGAATTCCACGTCTATCTGAACG-3′	this study
*ppsR*1 R	5′-CGGATCCACTGTTACTCATCGGCTCCG-3′	this study
*ppsR*2 F	5′-CGGGTACCTCCTTAAGAACCCGTC-3′	this study
*ppsR*2 R	5′-TGTCTAGACACTCAATCCTCTGCG-3′	this study
12up	5′-CCACGATGCCTTGCGTCA GG-3′	this study
12down	5′-GCTGACGACCAGAAGCGCGC-3′	this study
lacZ in	5′-AAAACTTTCAGTGCCGCCAGC-3′	this study
lacZ out	5′-CAG CAT TTT CTC TGG CTC-3′	this study
RPA1528 F	5′-TGAAGGAAGGTGGCTGGTGGCT-3′	this study
RPA1528 R	5′-AGCAGGATCGCGGAAGCGAA-3′	this study
RPA1542 F	5′-CGGCATCGAGACCACCTTCACC-3′	this study
RPA1542 R	5′-ATCTTCCACCACATCGGCGAGC-3′	this study
RPA1549 F	5′-CGCGCATCCTACGTTCTGCTGT-3′	this study
RPA1549 R	5′-TTTGCGCCTTCACTGCCTCG-3′	this study
RPA1554 F	5′-GACGAGCTGAACCATGCCTCGA-3′	this study
RPA1554 R	5′-ACTCGAACGCCACCAGCTTCG-3′	this study
RPA3250 F	5′-CGCATCCTCAGAAACGCGGA-3′	this study
RPA3250 R	5′-AAGAGAAGAACGGCTACGTGGCG-3′	this study

[a] Abbreviations: Km, kanamycin; Gm, gentamycin.

with halogen lamps (Capsylite, Sylvania) at an intensity of 150 μmol m^{-2} s^{-1}, measured with a photometer equipped with an LI-190SB quantum sensor (LI-COR Inc.). Cultures underwent 2.5−3 mass doublings before being harvested by centrifugation at a turbidity of 105−115 Klett units (∼10^9 cfu/mL). *Escherichia coli* strains were grown at 37 °C in Luria-Bertani medium, supplemented with 20 μg/mL gentamicin when appropriate for plasmid selection.

Spectroscopy. Absorption spectroscopy of intact cells was performed as described previously (*20*), and data were collected with a TIDAS II spectrophotometer (J&M Analytische Mess- und Regeltechnik). Light scattering at 650 nm was used to normalize the spectra, and the data from three independent cultures were averaged.

Peak Deconvolution. Deconvolution of the overlapping spectral components arising from LH1, LH2, and LH4 complexes was performed with Grams 32 AI (6.00) (Galactic). The background was removed by fitting of a polynomial baseline followed by fitting of the photosynthetic complex components using a mixed Gaussian/Lorentzian function. It was assumed that the LH1/RC absorption is dominated by LH1 and can be modeled by a single peak. The LH4 and LH2 contributions to the 808 nm peak were estimated by assuming that a pure LH2 sample has an 808 nm to 862 nm absorption ratio of approximately 0.7 (*3*).

Cell Fractionation. Cells from aerobically dark grown *R. palustris* cultures were pelleted, resuspended in 50 mM Tris-HCl buffer (pH 8.0), disrupted using a Bead beater, and centrifuged at 25800*g* for 10 min. The supernatant was centrifuged at 412000*g* for 14 min to pellet membrane vesicles (chromatophores). The resuspended pellet and supernatant were centrifuged a second time, yielding the membrane fraction. Samples were stored at −80 °C for Western blots.

Western Blotting. Chromatophores (20 μg of protein) as determined by a protein assay (Pierce) with BSA as the test standard were mixed with SDS−PAGE sample buffer (*21*) and heated at 95 °C for 1 min. Empirically determined amounts of pure RCs from *Rh. sphaeroides* (0.2 μg) were treated the same way. Samples were separated via SDS−PAGE (12% acrylamide) and transferred to membranes, and the RC M protein was detected as recommended in the ECL Western blotting kit (Amersham Biosciences) by using rabbit antisera raised against purified *Rh. sphaeroides* RC M protein. The signals were quantified using ImageJ (http://rsb.info.nih.gov/ij/).

DNA Manipulations. Standard protocols were used for cloning and transformations. Chromosomal DNA was purified using the Puregene DNA isolation kit from Gentra Systems. PCR was performed with Herculase enhanced DNA polymerase (Stratagene). DNA fragments were excised and purified using the Qiagen Qiaquick extraction kit. Plasmid DNA was purified with the Qiaprep spin miniprep kit. DNA sequencing was performed at the University of Iowa DNA core facility using standard automated sequencing methods.

Transposon Mutagenesis. pUTmini-Tn5 *lacZ*1 (*22*) was used to mutagenize *R. palustris* CGA009. The plasmid contains a mini-transposon harboring a Km resistance gene and a promoter-less *lacZ* gene. Cultures of *R. palustris* CGA009 and *E. coli* S17−1(λ-pir)(pUTminiTn-5 *lacZ*1) that were in the exponential phase of growth were mixed in a recipient to donor ratio of 4:1, and conjugations were performed as described previously (*23*). PM plates containing succinate and Km were used to select for *R. palustris* mutants possessing a mini-transposon insertion. A subset of those *R. palustris* transposon mutant strains that differed in color from the parental strain when grown on agar plates in air was collected and spotted to a grid on PM plates containing succinate and Km.

Identification of Transposon Insertion Sites. Arbitrary PCR (*24*) was used to identify sequences flanking the transposon using primers [*lacZ* in and *lacZ* out (Table 1)] unique to the *lacZ* sequence. Arbitrary primers and conditions for PCR were as previously described (*25*). PCR products were purified from agarose gels and used for sequencing with the *lacZ* out primer.

The location of the sequence flanking the transposon within the *R. palustris* genome and the orientation of the transposon in relation to the interrupted gene were determined using the *R. palustris* genome project web site (http://genome.ornl.gov/microbial/rpal/) and Artemis genome-viewing software (*26*).

Complementation of PpsR Mutant Strains. The *ppsR* genes were amplified from CGA009 using PCR primer pairs [*ppsR*1 F/R and *ppsR*2 F/R (Table 1)] to produce DNA segments including 262 (*ppsR1*) and 322 (*ppsR2*) base pairs 5′ of the start codon to increase the likelihood of retaining the *R. palustris* native promoter. Products were purified from agarose gels, digested with the appropriate restriction endonucleases, and ligated into *Eco*RI/*Bam*HI- and *Kpn*I/*Xba*I-digested pBBR1MCS-5 (*27*) for cloning of *ppsR*1 and *ppsR*2, respectively. The resultant plasmids were called pBB001 (*ppsR1*) and pBB002 (*ppsR2*), respectively. *E. coli* S17−1 was transformed and used for the transfer of the plasmids by conjugation (*23*) into the respective mutant strain.

Amplification and Alignment of ppsR Sequences from Various R. palustris Strains. Primers [12up and 12down (Table 1)] were designed to amplify 400 bp regions of *ppsR*2 from nine *R. palustris* strains that were isolated from sediment samples from The Netherlands or the United States by direct plating (*28*−*32*). The *ppsR*2 gene was also amplified from *R. palustris* strains CEA001 and CGA009, which were both derived from the culture collection of R. Clayton (Cornell University, Ithaca, NY) years ago. The amplified fragments extend from base pair 1116 through the stop codon of the *ppsR*2 sequence. PCR products were separated on agarose gels, excised, purified, and sequenced with the 12up primer (Table 1). Alignment of the retrieved sequences was achieved using ClustalW (*33*).

Sequence Analysis. The PpsR putative binding sites in the 5′ regions of photosynthesis genes were identified with ELSEA (http://www.entu.cas.cz/mach/elsea/elsea.html).

Overview of Microarray Experiments. A whole genome microarray was constructed using a 70mer-based platform designed using ArrayOligoSelector to minimize cross-hybridization among probes (*34*). More than 99% of the *R. palustris* genome was represented by the oligonucleotides, spotted in duplicate onto glass slides. Each *R. palustris* culture of parental strain CGA009 and *ppsR* mutant strains PPSR1$^-$ and PPSR2$^-$ was grown in triplicate under aerobic conditions to mid-log phase. Cultures were added to centrifuge bottles containing crushed ice and harvested by centrifugation. The cell pellets were stored at −80 °C for RNA isolation at a later time. Thawed cells were disrupted by bead beating and total RNA extracted using the RNAeasy kit (Qiagen), including DNase treatment on the columns.

Probe Design and Microarray Spotting. The software code of ArrayOligoSelector (http://arrayoligosel.sourceforge.net/) was modified for choosing acceptable probes toward the center of each gene coding region, allowing RNAs to be amplified using a random priming method. 70mer probes were spotted onto UltraGAPS slides (Corning) at 40 pmol/μL in 3× SSC buffer using a Virtek ChipWriter Pro robotic arrayer (Bio-Rad).

RNA Labeling. Total RNA (60 μg) was diluted in water to 15.5 μL, and 3 μL of random hexamer (3 μg/μL) (Amersham Biosciences) was added. The samples were heated to 70 °C for 10 min followed by rapid cooling on ice. Aliquots of 6 μL of 5× First-Strand buffer (Invitrogen), 3 μL of 0.1 M DTT, and 0.7 μL of a 50× mix of NTPs (25 mM dATP, dGTP, and dCTP, 10 mM dTTP, and 15 mM amino allyl dUTP) (Ambion) were added to the samples, which were then heated to 42 °C for 2 min. SSIII reverse transcriptase (2 μL) (Invitrogen) was added to initiate cDNA synthesis at 42 °C for 1 h followed by an additional hour at 50 °C. After reverse transcription, the RNA was hydrolyzed and the sample purified and labeled using aliquots of Cy3 or Cy5 Mono Reactive Dye (Amersham Biosciences) as described previously (*35*).

Hybridization, Scanning, and Data Analysis. Microarray processing conditions were optimized for accommodation of the GC-rich sequence of the *R. palustris* genome. We found that hybridization temperatures above 55 °C were necessary to reduce the level of nonspecific binding of target cDNA to the probe set (*36*). In turn, the more stringent incubation temperatures reduced the signal intensity of the microarray to near-background levels. Consequently, the indirect amino allyl labeling was chosen to increase the frequency of incorporation of fluorescent nucleotides in the target cDNA to levels well above the observed background. To minimize error associated with biological and experimental variation, microarray hybridizations were designed using previously reported guidelines (*37*, *38*).

UltraGAPS microarray slides (Corning) were prepared for hybridization by being hydrated briefly under steam and being snap dried on a heater block, followed by cross-linking with 600 mJ of UV in a Stratalinker 1800 instrument (Stratagene). Slides were blocked using BSA according to the manufacturer's protocol and dried in a tabletop centrifuge.

Concentrated labeled cDNA samples were suspended in 60 μL of Pronto cDNA/long oligo hybridization buffer (Corning), and 29 μL was applied to the microarray slide (*ppsR* mutant vs parental cDNA) and overlaid with a 40 mm × 22 mm coverslip (Schleicher and Schuell). The slides were placed in a hybridization chamber (Monterey Industries) and incubated in a water bath overnight at 55−58 °C. Hybridization slides were washed for 5 min in 2× SSC and 0.1% SDS (55 °C), followed by a 5 min wash in 0.1× SSC and 0.1% SDS (room temperature) and two 3 min washes in 0.1× SSC. Slides were dried by centrifugation in a tabletop centrifuge at 2000 rpm for 5 min and scanned using a Virtek Chipreader (Bio-Rad). Triplicate microarray slides were run for each experiment consisting of a hybridization of independently grown mutant strain cDNA versus CGA009. Where enough RNA sample was available, an additional repeat of each biological replicate was performed. Additionally, a calibration experiment was performed in which RNAs from the various mutant and CGA009 cultures were pooled, split, reverse transcribed, and labeled with either Cy3 or Cy5. The Cy3- and Cy5-labeled cDNAs from the identical pools of RNA template were then cohybridized to two slides to obtain reference distributions for technical variations. Images were processed using Imagene (Biodiscovery Inc.). The lcDNA software package was used for data normalization and to assess the statistical confidence of gene expression values (*37*, *38*). Genes whose ratios (*ppsR* mutant:CGA009) of expression were ≥2, and whose statistical confidence scores were ≥0.95, were considered to be expressed at significantly greater levels in the mutant strains.

Real-Time RT-PCR. First-strand cDNA synthesis was performed according to Invitrogen's protocol with 150 ng of random hexamers, 150 ng of total *R. palustris* RNA, and 2 μL of SSIII reverse transcriptase. Samples of the RNA used in the microarray experiments were reverse transcribed for 10 min at room temperature, 20 min at 42 °C, and 1 h at 48 °C, followed by enzyme inactivation at 70 °C for 20 min. Reaction mixtures were diluted 3-fold with water upon completion. Real-time PCR was performed with gene-specific PCR primers designed using MyPROBES software for *pufM*, *bchN*, *puhB*, *hemA*, and RPA3250 (*35*). The reactions were conducted on a Smart Cycler (Cepheid) with 2 μL of cDNA added per 25 μL of real-time PCR sample using the QuantiTect SYBR green PCR kit (Qiagen). A four-step program consisting of denaturation, annealing, extension, and data acquisition was used. The specificity of RT-PCR primers was determined using a melt curve after the amplification to show that only a single species of qPCR product resulted from the reaction. Additionally, a control experiment was performed in which a sample of RNA, equal to the amount added to the RT reaction mixture, was used as a target in a qPCR reaction with gene-specific probes. The sample was determined to be free of DNA contamination because of the absence of any amplification product. Calibration curves were performed for each primer pair using genomic DNA template amounts over 4 orders of magnitude, starting at approximately 4700 genome copies and increasing to ~4.7×10^6 copies. Calibration curves with linearity R^2 values of at least 0.98 were used to determine the fold changes of the mutant strains relative to parental strain CGA009. Data were normalized to the amplification product of primers for *rplC* (RPA3250), a ribosomal protein gene with medium to high microarray signal intensity, which showed no significant changes in expression across all the microarray experiments.

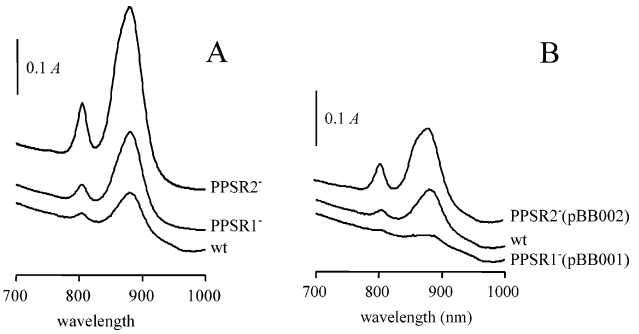

FIGURE 2: Absorption spectra of cells grown under high aeration. LH1 absorbs at 880 nm; LH2 complexes absorb at 808 and 862 nm, and the LH4 complex absorbs at 808 nm. *A* is absorbance. (A) Absorption spectra of CGA009 (WT) and mutant strains PPSR1⁻ and PPSR2⁻. (B) Absorption spectra of CGA009 (WT) and mutant strains complemented in trans with *ppsR1* (pBB001) or *ppsR2* (pBB002) genes.

Table 2: Relative Increases in Absorbance in Mutant Strains Grown at Various Oxygen Concentrations

	increase in absorbance relative to that of CGA009[a]				
	high pO_2			low pO_2	PS[b]
strain	808 nm	862 nm	880 nm	880 nm	880 nm
PPSR1⁻	1.9	2.0	2.0	1.3	1.0
PPSR2⁻	6.6	4.8	3.9	2.1	1.3

[a] Values obtained from the averaged spectra shown in Figure 2A. [b] Anaerobic, photosynthetic growth.

RESULTS

Absorption Spectra of PpsR Mutants and Complemented Strains. A representation of the *ppsR* region of the chromosome of *R. palustris* CGA009 is given in Figure 1B and shows the locations of the *ppsR1* and *ppsR2* mutations. Previous experiments on *R. palustris* revealed that the LH2 and LH4 complexes each produce an 808 nm absorption peak, and the LH2 862 nm and LH1 880 nm peaks overlap (*3*, *17*, *39*), making quantitatively rigorous attribution of in vivo peaks difficult. However, the relative contributions can be semiquantitatively deduced by inspection of peak shapes, and amplitudes at the wavelengths absorbed by these complexes (*17*). The RC contributes less than 10% to the in vivo absorption and so is not considered in our spectral analyses. We first present the raw absorption spectra in Figure 2, with relative absorption values summarized in Table 2, and give a more detailed analysis of peak compositions in the Discussion.

(i) High-Aeration Cultures. Parental strain CGA009 had relatively small absorption peaks in the 700−1000 nm range (Figure 2A), which in principle could be due to a combination of LH4 (808 nm), LH2 (808 and 862 nm), and LH1 (880 nm) (*17*). We attribute the observed peaks mainly to LH1 and LH2. The *ppsR1* mutation significantly increased the amplitude of these peaks, with little change in peak shapes (Figure 2A and Table 2). This indicates that the PpsR1 protein represses the expression of genes that encode BChl biosynthetic enzymes (*bch* genes), and/or the structural proteins of LH2 (*puc* genes) and LH1 (*puf* genes). The *ppsR2*

mutation resulted in even greater increases in the peak amplitudes in this region of the absorption spectrum and also appeared to increase the amount of LH2 relative to LH1. This is because the ratio of 862 nm absorbance relative to 880 nm absorbance increased, as indicated by the shoulder at 862 nm of the long wavelength peak (Figure 2A and Table 2). The ratio of 808 nm to 862 nm absorbance in the *ppsR2* mutant was greater than that of both CGA009 and the *ppsR1* mutant, indicating an increased amount of LH4 (Table 2). These data indicate that the PpsR2 protein, like PpsR1, represses the expression of genes needed for formation of photosynthetic pigment−protein complexes, but the regulation of LH complexes by PpsR2 differs quantitatively and qualitatively from PpsR1 regulation.

(ii) Complementation of ppsR1 and ppsR2 Mutations. The *ppsR1* mutation was complemented in *trans* with plasmid pBB001, which contains the *ppsR1* coding region and 5′ sequences extending to 9 bp 3′ of the stop codon of the congruently transcribed *pufM* gene (Figure 1B). Cells of the resultant strain PPSR1$^-$(pBB001) had very small absorption peaks when grown with high aeration (Figure 2B). The *ppsR2* mutation was similarly complemented with plasmid pBB002, which contains the *ppsR2* gene and sequences extending to 8 bp 5′ of the start codon of the divergently transcribed *cycA* gene (Figure 1B). The resultant strain PPSR2$^-$(pBB002) had significantly smaller absorption peaks than the noncomplemented *ppsR2* mutant (Figure 2A). The absence of restoration of absorption peaks in strains PPSR1$^-$(pBB001) and PPSR2$^-$(pBB002) to exactly the parental strain CGA009 values is attributed to the unnatural location of the complementing genes on plasmids, resulting in an increase in gene copy number, and possible differences in promoters and rates of mRNA degradation. Regardless, these data indicate that the increases in absorption peak amplitudes in cells containing chromosomal disruptions of *ppsR* genes and grown with high aeration were due to the loss of the respective PpsR protein, because the peaks decreased in magnitude in *trans*-complementation.

(iii) Low-Aeration and Anaerobic (photosynthetic) Cultures. When parental strain CGA009 was grown with low aeration, the magnitudes of the absorption peaks increased by 6-fold (808 nm), 4-fold (862 nm), and 2-fold (880 nm), compared to high-aeration cultures (not shown). Growth of the two PpsR mutants under low-aeration conditions resulted in smaller differences in these peak amplitudes relative to the parental strain, and anaerobic (photosynthetic) growth nearly abolished these differences (Table 2).

Taken together, the absorption spectra indicate that PpsR1 and PpsR2 each function to repress photosynthesis gene expression in response to the presence of O_2. These two proteins appear to repress expression of some of the same photosynthesis genes to different degrees or to have slightly different profiles in terms of the genes that are regulated.

Western Blot Analysis of R. palustris CGA009 and PpsR Mutant Strains. The production of the RC M protein in CGA009 and mutant strains PPSR1$^-$ and PPSR2$^-$ was evaluated in a Western blot experiment, using *Rh. sphaeroides* RC M antiserum (Figure 3). This antiserum reacts specifically with a purified *Rh. sphaeroides* RC sample (lane 1). Using equal amounts of chromatophore samples from aerobically grown *R. palustris* wild-type and mutant strains, we obtained two bands which migrate to a slightly higher molecular weight position than the *Rh. sphaeroides* RC sample. The relative intensities of the two bands in lanes 2−4 were constant, and quantification of the total signal intensities revealed a 1.9-fold (PPSR1$^-$) and 3.4-fold (PPSR2$^-$) increase compared to the wild-type level. Therefore, we suggest an increase in RC production similar to the LH peak increases in the two PpsR mutants.

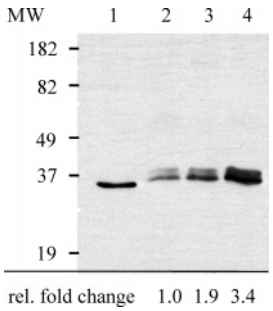

FIGURE 3: Western blot probed with the *Rh. sphaeroides* RC M antibody: lane 1, purified *Rh. sphaeroides* RC (control, 0.2 μg loaded); lane 2, chromatophores from *R. palustris* CGA009; lane 3, chromatophores from *R. palustris* PPSR1$^-$; and lane 4, chromatophores from *R. palustris* PPSR2$^-$. *R. palustris* strains were grown as described in the legend of Figure 2, and 20 μg of total protein was loaded per lane. The intensities of the signals were quantified and given as relative fold change of the wild-type signals (lane 2). MW means molecular weight.

Transcriptome Analysis of PpsR Mutants and PpsR Binding Sites. Although the absorption spectra indicated that PpsR1 and PpsR2 repress the amounts of photosynthetic complexes in cells grown under high-aeration conditions, these experiments did not reveal exactly which genes are repressed. It was also unclear whether PpsR1 and PpsR2 repress different sets of genes or the same genes to different degrees. To address these questions, we used transcriptomics to compare mRNA levels of selected genes between the PpsR mutants and parental strain CGA009, during growth with high aeration.

The total number of ORFs whose expression was affected in the PpsR mutants after application of the cutoff criteria described in Materials and Methods was limited to 23 for PPSR1$^-$ and 36 for PPSR2$^-$ (see the Supporting Information). For PPSR1$^-$, of eight derepressed ORFs, seven were related to photosynthesis, while in PPSR2$^-$, 22 of 31 upregulated ORFs were photosynthesis genes.

In general, the changes in the level of expression that we observed between parental and mutant strains were small but quantitatively similar to what was recently reported for a *Rh. sphaeroides* PpsR mutant (*10*). Because of the small changes, we take a conservative approach and, with the exception of the *pufM* gene, focus on those genes that belong to predicted operons that are preceded by closely spaced PpsR binding motifs. DNA footprinting experiments with PpsR-regulated genes from *Rhodobacter*, *Bradyrhizobium*, and *Rhodopseudomonas* species revealed that PpsR proteins from these species bind to the quasi-conserved motif 5′-TGTgaN_8tgACA-3′, typically present as a repeat separated by 7−8 bp (reviewed in ref *4*). Regions of the CGA009 genome sequence encoding photosynthesis genes were scanned for closely spaced repeats of this motif, and the results are shown in Figure 4. The upward-pointing arrows in Figure 4A indicate the positions of closely spaced motif repeats, and the circles denote genes that were significantly

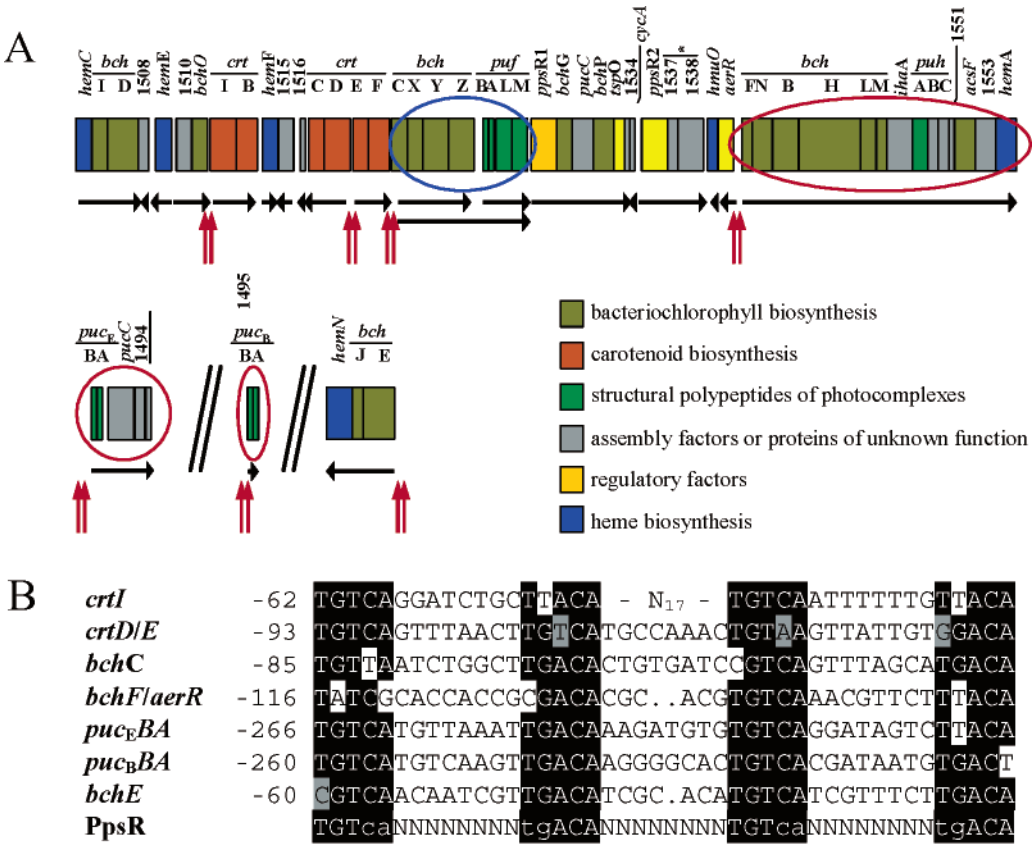

FIGURE 4: Organization of photosynthesis genes and regulation by PpsR proteins. (A) Photosynthesis gene cluster, *puc*$_B$*BA*, *puc*$_E$*BAC*-1495, and *bchEJ-hemN* genes. Closely spaced PpsR binding motifs are denoted with red vertical arrows. Potential operons, defined as clusters of congruently transcribed genes, are denoted with black horizontal arrows; an additional arrow is added to indicate transcription read-through from *bchCXYZ* into *pufBALM*. Using a cutoff of ≥2-fold and ≥95% confidence, genes encircled in red were derepressed in *ppsR1* and *ppsR2* mutants, while genes encircled in blue passed the cutoff criteria for only strain PPSR2$^-$. Asterisk denotes the frameshifted *bphB* pseudogene in strain CGA009 (*1*). (B) Alignment of the potential PpsR binding sequences denoted with red vertical arrows in panel A. Negative numbers give the distance in nucleotides from a start codon. Nucleotides that are identical to those in the PpsR consensus sequence are shown as white letters outlined with black. Nucleotides that differ from the consensus and may reduce the affinity for PpsR proteins are shown as black letters outlined with gray. Dots indicate a gap introduced for optimal alignment. N_{17} represents the 17-base spacing between the *crtIB* motifs. PpsR is the consensus sequence for PpsR binding (5′-TGTcaN$_8$tgACA-3′), with lowercase letters indicating weaker conservation (*4*).

derepressed in PpsR mutants. All of the encircled genes contain the motif repeat located 5′ of the start codon of the first gene of predicted operons except for *pufBALM*, which was found to be derepressed ≥2 fold only in PPSR2$^-$. However, derepression of *puf* operon expression may be due to "superoperonal" transcription readthrough from the PpsR-regulated *bchCXYZ* operon located 5′ of the *puf* genes (Figure 4A), as observed in *Rh. capsulatus* (*40*, *41*) and perhaps *Rh. sphaeroides* (*10*). The repeat located 5′ of *crtIB*, although well conserved in terms of two 5′-TGTcaN$_8$tgACA-3′ sequences, has these sequences separated by 17 bp instead of the usual 7−8 bp. The *bchEJ-hemN* putative operon, which is located elsewhere on the chromosome and contains a 5′ PpsR binding motif repeat, was not significantly derepressed in the PpsR mutant strains. However, this motif shows a substitution of a C in place of an otherwise conserved T (Figure 4B). Similar differences in sequence composition and spacing of repeats have been found to have significant effects on PpsR binding in other species (reviewed in ref *4*), and so we suggest that the motif sequence differences noted above explain the observed differences in the regulation of these genes.

Specific levels of derepression are given in Table 3. Listed genes not passing the cutoff criteria (np) exhibited a mean of ≥1.6-fold upregulation within a ≥95% confidence interval. Although the expression changes for the *pufBALM* and *bchCXYZ* operons in strain PPSR1$^-$ are slightly beneath the cutoff criteria (Supporting Information), these microarray data indicate that the *R. palustris* PpsR1 and PpsR2 proteins repress transcription of the same subset of photosynthesis genes, but to different degrees that are consistent with the absorption spectra and the Western blot result. In general, the *ppsR2* mutation had a greater derepressive effect than the *ppsR1* mutation. For example, the *puc*$_B$*BA* and *puc*$_E$*BA* gene sets encoding LH2 proteins are preceded by PpsR binding sites and were derepressed 2.1-fold in the *ppsR1* mutant, and 4.1−6.3-fold in the *ppsR2* mutant. A similar pattern exists for genes of the *bchF* to *hemA* putative operon (≤2.3-fold for PPSR1$^-$ and 3.3−4.7-fold for PPSR2$^-$).

Quantitative RT-PCR. To further validate the microarray data, segments of four mRNAs encoding photosynthesis-related proteins (*pufM*, *bchN*, *hemA*, and *puhB*) were chosen for RT-PCR analysis. RT-PCR primers (Table 1) were designed to minimize amplification of nonspecific transcripts, and data were normalized using the control transcript of RPA3250 (*rplC*), a ribosomal protein gene with medium to high microarray signal intensity that did not differ across the microarray experiments. In each case, the mean fold

Table 3: Effects of *ppsR* Mutations on the High Aeration Level of Expression of Selected Photosynthesis-Related Genes that Are Preceded by Closely Spaced PpsR Binding Motifs

putative operon and **gene**[a]	function	fold change[b] PPSR1$^-$	fold change[b] PPSR2$^-$
puc$_B$***BA***			
puc*$_B$*A	LH2 pigment binding protein α	np	3.1 (2.5−3.9)
puc*$_B$*B	LH2 pigment binding protein *β*	2.1 (1.4−3.2)	4.1 (2.7−5.8)
puc$_E$***BA****C*-1494-**1495**			
puc*$_E$*A	LH2 pigment binding protein α	2.0 (1.5−2.9)	6.3 (2.2−21.0)
puc*$_E$*B	LH2 pigment binding protein *β*	2.1 (1.5−3.1)	4.5 (3.2−6.1)
RPA**1495**	unknown protein	2.3 (1.7−3.1)	4.0 (3.0−5.4)
bchCXYZ	bacteriochlorophyll synthesis	np	2.5 (2.1−3.0)
pufBALM[c]	reaction center M subunit	np	2.7 (2.0−3.7)
*bchFN****B****HLH-lhaA-puhA****B****C*-1551-***acsF***-1553-*hemA*			
bchB	bacteriochlorophyll synthesis	np	3.4 (1.6−7.6)
puhB	PS complex assembly	np	4.7 (3.0−7.2)
acsF	bacteriochlorophyll synthesis	2.3 (1.4−4.0)	3.3 (2.4−4.4)

[a] Selected photosynthesis genes (bold) whose expression is affected in three independent biological replicates with a statistical confidence of ≥95% and a fold change of ≥2.0. [b] Fold change expressed as normalized signal intensities of Cy5 (PpsR mutant) against Cy3 (CGA009). Values in parentheses give the range of fold changes where the average expression is ≥95% likely to be found. The term np indicates values with a statistical confidence of ≥95% and fold changes of ≥1.6− <2.0. [c] The *pufBALM* operon is not preceded by a PpsR binding motif repeat but may be transcribed from the *bchCXYZ* promoter. PS means photosynthetic.

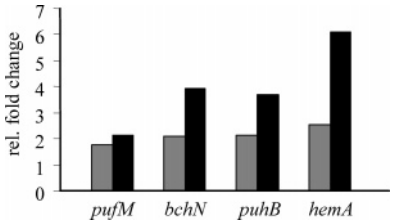

FIGURE 5: Expression changes of selected photosynthesis genes in PPSR1$^-$ and PPSR2$^-$ as assayed by RT-PCR. The relative fold changes in expression under high-aeration growth of mutant strains compared to CGA009 are shown: gray bars, PPSR1$^-$; black bars, PPSR2$^-$. RT-PCR expression values are derived from at least three separate amplifications. The standard deviation in all measurements did not exceed 29%.

CGA009	AAC TGC TAC
355	AAC TGC TAC
HAA3	AAC TGC TAC
CEA001	AAC CGC TAC
API	AAC CGC TAC
NCIMB8288	AAC CGC TAC
BIS3	AAC CGC TAC
DCP3	AAC CGC TAC
RCH500	AAC CGC TAC
BISA52	AAC CGC TAC
BISA14	AAC CGC TAC

FIGURE 6: Alignment of *ppsR2* sequences from various *R. palustris* strains. The sequence starts at base pair 1312 (codon 438) and extends to codon 440 of the *ppsR2* sequence. The single nucleotide change that results in the substitution of a Cys for an Arg at position 439 is shown as white letters outlined with black.

change for a given gene measured by RT-PCR corroborated the data determined by microarray analysis (Figure 5 and Supporting Information). These results confirm that the microarray data reflect genuine differences in the relative amounts of mRNAs.

Natural Sequence Variation of Codon 439 in the ppsR2 Gene. It was proposed that the *ppsR2* gene of *R. palustris* CGA009 has undergone a mutation as a result of laboratory propagation for many years, changing the Arg 439 codon to a Cys codon (CGC → TGC) and rendering the PpsR2 protein incapable of binding to the conserved motif repeat (see above) bound by other PpsR proteins (*14*). We PCR-amplified and sequenced 400 bp segments of *ppsR2* genes from 11 independent isolates of *R. palustris* (Table 1) and found these *ppsR2* sequences are identical except for codon 439. Eight of the strains encode Arg at this position, but in addition to strain CGA009, the relatively recently isolated strains 355 and HAA3 encode Cys (Figure 6). These data, along with the results described above showing that PpsR2 of CGA009 is a functional repressor, indicate that there is a natural polymorphism at *ppsR2* codon 439 that results in either Cys or Arg at this position without inactivation of the repressor activity of this protein.

DISCUSSION

The *Rhodobacter* species and *Ru. gelatinosus* each have a single *ppsR* gene (*4*); however, the *Ru. gelatinosus* PpsR protein was proposed to function as both a repressor and an inducer (*5*), whereas the *Rhodobacter* PpsR proteins appear to be solely repressors of gene transcription (*10*, *12*, *42*). In this study, we found that the PpsR1 and PpsR2 proteins of *R. palustris* CGA009 function as repressors of genes required for photosynthesis, evidently in response to O_2. This is contrary to the situation in the closely related *Bradyrhizobium* strain ORS278, where the PpsR1 and PpsR2 proteins were reported to respond to anaerobiosis to activate gene expression (PpsR1), and in the absence of far-red light to repress photosynthesis gene expression (PpsR2) (*11*, *14*).

Functionality of PpsR2 Protein Variants. R. palustris strain CGA009 is more pigmented than strain CEA001 under aerobic growth conditions (ref *14* and our unpublished observations). To explain this difference, Giraud et al. (*14*) hypothesized that a mutation had occurred in the *ppsR2* gene of CGA009, resulting in an inactive repressor. Indeed, the CEA001 and CGA009 *ppsR2* genes differ by a single nucleotide (Figure 6), a difference that results in a Cys in the CGA009 PpsR2 protein as opposed to an Arg in the CEA001 PpsR2 protein at amino acid 439, located in the predicted DNA-binding (HTH) region (see Figure 1A). DNA footprint analyses using heterologously expressed, His-tagged PpsR2 proteins from strains CGA009 and CEA001 indicated protection of the *crtI* promoter region of CEA001 from DNase digestion only with PpsR2 of CEA001 (*14*). The failure of CGA009 His-tagged PpsR2 to protect the CEA001

crtI promoter region was offered as evidence that the strain CGA009 protein is nonfunctional (*14*). Although it is possible that the observed Cys/Arg variation within the otherwise identical HTH region of PpsR2 affects its binding affinity for some nucleotide sequences, our data clearly show that PpsR2 of CGA009 is a functional repressor. We suggest that the 17 bp separating the *crtIB* PpsR binding motif repeats in CGA009 reduces the affinity for PpsR2, which is consistent with our microarray data.

Significance of PpsR Cys Residues. The role of Cys residues in PpsR proteins appears to differ between species, and perhaps within strains of the same species. In *Rhodobacter* species, a critical role of an intramolecular disulfide bond for the binding of PpsR to the characteristic motif was reported for *Rh. capsulatus* and *Rh. sphaeroides* (*6*, *7*), but in *R. palustris* CGA009, only PpsR1 would be capable of intramolecular disulfide bond formation (involving Cys 6, Cys 247, or Cys 384), because PpsR2 contains a single Cys at residue 439 (Figure 1A). It is possible that reduction of the single Cys residue in CGA009 PpsR2 breaks an intermolecular disulfide bond to cause a decreased affinity for the PpsR binding DNA sequence motifs located 5′ of PpsR2-regulated photosynthesis genes, as part of an O_2 signaling pathway. Additional experiments are needed to evaluate the validity of this speculation.

Correlation of PpsR-Regulated Genes, Absorption Spectra, and RC Protein Levels. In a genome-wide transcriptome analysis of *Rh. sphaeroides*, Moskvin et al. (*10*) observed the presence of two closely spaced motifs 5′ of PpsR-regulated genes. Our bioinformatic analysis of *R. palustris* CGA009 photosynthesis genes revealed similar tandem motifs 5′ of a number of genes that according to our transcriptome analysis are regulated by PpsR1 and PpsR2 (Figure 4). We suggest that expression of all of these genes is under direct control of the PpsR1 and PpsR2 repressors. We found closely spaced PpsR binding motifs located 5′ of the LH2-encoding *puc*$_B$*BA* and *puc*$_E$*BA* genes, and the transcriptome data in Table 3 indicate that these genes were repressed by PpsR1 and PpsR2. Our transcriptome data also indicated that the expression of *puc*$_A$*BA* and *pucCB* operons encoding LH2 peptides and the *puc*$_D$*BA* operon encoding LH4 peptides is controlled by the PpsR proteins (see the Supporting Information). This could be a biologically significant result; however, plausible, closely spaced PpsR binding motif repeats were not found 5′ of these genes, and we cannot rule out the possibility that there was cross hybridization of *puc* cDNAs in the microarray experiments. The five *puc* operons have very similar nucleotide sequences (*1*), so the *puc* gene segments represented by oligonucleotide probes had a level of sequence identity of ≥60% between *pucA* orthologues and ≥80% between *pucB* orthologues.

The absorption spectra (Figure 2 and Table 2) clearly show that PpsR1 and PpsR2 repress the formation of LH complexes, but because the peaks of LH1, LH2, and LH4 complexes overlap, it is difficult to make quantitative assignments of absorption at specific wavelengths to specific LH complexes. Therefore, we used published information about the absorption spectra of LH1, LH2, and LH4 complexes (*3*, *17*, *39*) in mathematical analyses to quantitatively "deconvolute" the overlapping LH peaks of cells grown with high aeration (Figure 7). The similarity of the sum of the computed peaks to the measured absorption

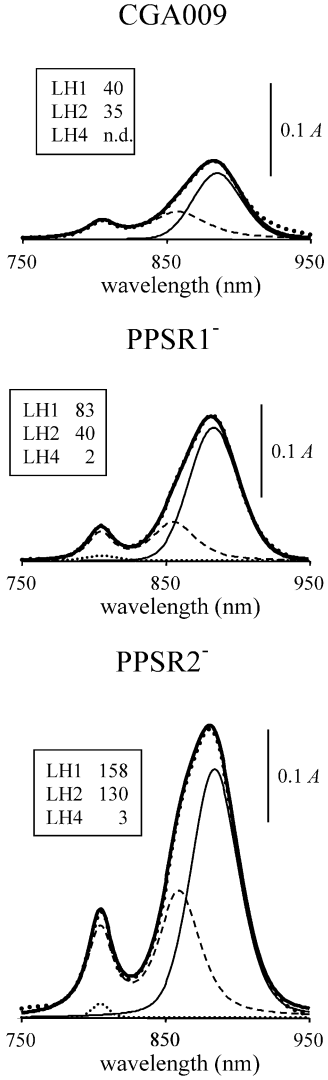

FIGURE 7: Mathematical deconvolution of LH absorption spectra of *R. palustris* cells grown under high-aeration conditions. The simulated absorption spectra (thick solid line) are composed of the three types of LH complexes: LH1 (thin solid line) absorbing at 880 nm, LH2 (dashed line) absorbing at 808 and 862 nm, and LH4 (line of small dots) absorbing at 808 nm. The measured in vivo absorption spectra are shown as lines made up of large dots. The computed area of each LH complex peak is given in the boxes. *A* is the absorbance; n.d. means the value was below the limit of detection.

spectra indicates a high degree of confidence. On the basis of these results (Figure 7), the parental strain CGA009 produced LH1 and LH2, with no contribution from LH4. The *ppsR1* mutation increased the amount of LH1, with a slight increase in the amounts of LH2 and LH4. The *ppsR2* mutation resulted in a relatively great increase in the amounts of LH1 and LH2, and an increase in the amount of LH4. However, the observed effects of *ppsR* mutations on the amounts of LH complexes may reflect a combination of direct, PpsR-mediated effects on the transcription of genes encoding LH protein components and indirect effects through other factors that affect LH complex levels (see below). Indirect effects such as PpsR regulation of a gene that in turn affects expression of LH4 may explain the changes in the small amounts of LH4, encoded by the *puc*$_D$*BA* genes that lack a closely spaced PpsR binding motif repeat. However, the peak attributed to LH4 could include RC absorbance. Since the RC contributes less than 10% to the

in vivo absorption spectra, we used a Western blot approach to evaluate the RC M protein levels in *R. palustris* CGA009 and the PpsR mutant strains. The 1.9-fold (PPSR1$^-$) and 3.4-fold (PPSR2$^-$) increases in RC M production are in line with our transcriptional data (Figure 5 and Table 3) and suggest that inactivation of *ppsR1* and *ppsR2* derepresses the expression of the *puf* operon.

A Model for PpsR1 and PpsR2 Function. We use the data presented here and in other publications to propose a model for PpsR1 and PpsR2 function in *R. palustris* CGA009 that differs from previous proposals (*11*, *14*) described in the introductory section, as follows. Each of the two PpsR proteins represses the transcription of photosynthesis genes during dark aerobic growth. Upon exposure of cells to far-red light, BphP undergoes a conformational change that, perhaps by direct interaction with one or both PpsR proteins, decreases the affinity of PpsR(s) for binding sites located 5′ of photosynthesis genes so that transcription of these genes is derepressed. In the absence of a functional BphP, PpsR(s) is light-insensitive and represses transcription in response to O_2 regardless of far-red illumination. This is the phenotype of *R. palustris* CGA009 (which is a *bphP* mutant).

Maximal derepression of photosynthesis genes during growth with high aeration occurred in the *ppsR2* mutant, whereas the *ppsR1* mutation resulted in a lower level of derepression. These phenotypic differences may reflect different affinities of PpsR1 and PpsR2 for PpsR binding sites, as well as the activities of other regulatory factors. The *R. palustris* genome encodes homologues of *regA*, *regB*, *aerR*, and *tspO* genes (*1*), all of which have been implicated in the regulation of photosynthesis gene expression in response to culture aeration in *Rhodobacter* species (*2*). Thus, there is the potential for superimposition of multiple O_2-dependent regulatory processes in *R. palustris*. Furthermore, the genome sequence of *R. palustris* indicates the production of several bacteriophytochromes (*1*), some of which have been shown to regulate photosynthesis gene expression in response to illumination (refs *16*−*18* and our unpublished work). These findings and the data presented in this paper indicate a complexity of photosynthesis gene regulation in *R. palustris* that differs significantly from that of other species of purple non-sulfur phototrophic bacteria.

ACKNOWLEDGMENT

We thank M. Kramar for contributions to the early stages of this work, M. Paddock for the purified *Rh. sphaeroides* RC, P. Jaschke for assistance in Western blotting, and M. Papiz and F. I. Rosell for help with peak deconvolution. The rabbit antisera raised against purified *Rh. sphaeroides* RC M protein were kindly provided by E. Abresch.

SUPPORTING INFORMATION AVAILABLE

Supporting microarray data. This material is available free of charge via the Internet at http://pubs.acs.org.

REFERENCES

1. Larimer, F. W., Chain, P., Hauser, L., Lamerdin, J., Malfatti, S., Do, L., Land, M. L., Pelletier, D. A., Beatty, J. T., Lang, A. S., Tabita, F. R., Gibson, J. L., Hanson, T. E., Bobst, C., Torres y Torres, J. L., Peres, C., Harisson, F. H., Gibson, J., and Harwood, C. S. (2004) Complete genome sequence of the metabolically versatile photosynthetic bacterium *Rhodopseudomonas palustris*, *Nat. Biotechnol. 22*, 55−61.
2. Zeilstra-Ryalls, J. H., and Kaplan, S. (2004) Oxygen intervention in the regulation of gene expression: The photosynthetic bacterial paradigm, *Cell. Mol. Life Sci. 61*, 417−436.
3. Tharia, H. A., Nightingale, T. D., Papiz, M. Z., and Lawless, A. M. (1999) Characterisation of hydrophobic peptides by RP-HPLC from different spectral forms of LH2 isolated from *Rps. palustris*, *Photosynth. Res. 61*, 157−167.
4. Elsen, S., Jaubert, M., Pignol, D., and Giraud, E. (2005) PpsR: A multifaceted regulator of photosynthesis gene expression in purple bacteria, *Mol. Microbiol. 57*, 17−26.
5. Steunou, A.-S., Astier, C., and Ouchane, S. (2004) Regulation of photosynthesis genes in *Rubrivivax gelatinosus*: Transcription factor PpsR is involved in both negative and positive control, *J. Bacteriol. 186*, 3133−3142.
6. Masuda, S., Dong, C., Swem, D., Setterdahl, A. T., Knaff, D. B., and Bauer, C. E. (2002) Repression of photosynthesis gene expression by formation of a disulfide bond in CrtJ, *Proc. Natl. Acad. Sci. U.S.A. 99*, 7078−7083.
7. Masuda, S., and Bauer, C. E. (2002) AppA is a blue light photoreceptor that antirepresses photosynthesis gene expression in *Rhodobacter sphaeroides*, *Cell 110*, 613−623.
8. Gomelsky, M., Horne, I. M., Lee, H.-J., Pemberton, J. M., McEwan, A. G., and Kaplan, S. (2000) Domain structure, oligomeric state, and mutational analysis of PpsR, the *Rhodobacter sphaeroides* repressor of photosystem gene expression, *J. Bacteriol. 182*, 2253−2261.
9. Penfold, R. J., and Pemberton, J. M. (1994) Sequencing, chromosomal inactivation, and functional expression in *Escherichia coli* of *ppsR*, a gene which represses carotenoid and bacteriochlorophyll synthesis in *Rhodobacter sphaeroides*, *J. Bacteriol. 176*, 2869−2876.
10. Moskvin, O. V., Gomelsky, L., and Gomelsky, M. (2005) Transcriptome analysis of the *Rhodobacter sphaeroides* PpsR regulon: PpsR as a master regulator of photosystem development, *J. Bacteriol. 187*, 2148−2156.
11. Jaubert, M., Zappa, S., Fardoux, J., Adriano, J.-M., Hannibal, L., Elsen, S., Lavergne, J., Vermeglio, A., Giraud, E., and Pignol, D. (2004) Light and redox control of photosynthesis gene expression in *Bradyrhizobium*: Dual roles of two PpsR, *J. Biol. Chem. 279*, 44407−44416.
12. Gomelsky, M., and Kaplan, S. (1995) Genetic evidence that PpsR from *Rhodobacter sphaeroides* 2.4.1 functions as a repressor of *puc* and *bchF* expression, *J. Bacteriol. 177*, 1634−1637.
13. Elsen, S., Ponnampalam, S. N., and Bauer, C. E. (1998) CrtJ bound to distant binding sites interacts cooperatively to aerobically repress photopigment biosynthesis and light harvesting II gene expression in *Rhodobacter capsulatus*, *J. Biol. Chem. 273*, 30762−30769.
14. Giraud, E., Zappa, S., Jaubert, M., Hannibal, L., Fardoux, J., Adriano, J.-M., Bouyer, P., Genty, B., Pignol, D., and Vermeglio, A. (2004) Bacteriophytochrome and regulation of the synthesis of the photosynthetic apparatus in *Rhodopseudomonas palustris*: Pitfalls of using laboratory strains, *Photochem. Photobiol. Sci. 3*, 587−591.
15. Braatsch, S., Gomelsky, M., Kuphal, S., and Klug, G. (2002) A single flavoprotein, AppA, integrates both redox and light signals in *Rhodobacter sphaeroides*, *Mol. Microbiol. 45*, 827−836.
16. Giraud, E., Zappa, S., Vuillet, L., Adriano, J.-M., Hannibal, L., Fardoux, J., Berthomieu, C., Bouyer, P., Pignol, D., and Vermeglio, A. (2005) A new type of bacteriophytochrome acts in tandem with a classical bacteriophytochrome to control the antennae synthesis in *Rhodopseudomonas palustris*, *J. Biol. Chem. 280*, 32389−32397.
17. Evans, K., Fordham-Skelton, A. P., Mistry, H., Reynolds, C. D., Lawless, A. M., and Papiz, M. Z. (2005) A bacteriophytochrome regulates the synthesis of LH4 complexes in *Rhodopseudomonas palustris*, *Photosynth. Res. 85*, 169−180.
18. Giraud, E., Fardoux, J., Fourrier, N., Hannibal, L., Genty, B., Bouyer, P., Dreyfus, B., and Vermeglio, A. (2002) Bacteriophytochrome controls photosystem synthesis in anoxygenic bacteria, *Nature 417*, 202−205.
19. Kim, M. K., and Harwood, C. S. (1991) Regulation of benzoate-CoA ligase in *Rhodopseudomonas palustris*, *FEMS Microbiol. Lett. 83*, 199−204.
20. Lilburn, T. G., Haith, C. E., Prince, R. C., and Beatty, J. T. (1992) Pleiotropic effects of *pufX* gene deletion on the structure and

function of the photosynthetic apparatus of *Rhodobacter capsulatus*, *Biochim. Biophys. Acta 1100*, 160−170.
21. Laemmli, U. K. (1970) Cleavage of structural proteins during the assembly of the head of bacteriophage T4, *Nature 227*, 680−685.
22. de Lorenzo, V., Herrero, M., Jakubzik, U., and Timmis, K. N. (1990) Mini-Tn5 transposon derivatives for insertion mutagenesis, promoter probing, and chromosomal insertion of cloned DNA in Gram-negative eubacteria, *J. Bacteriol. 172*, 6568−6572.
23. Egland, P., Gibson, J., and Harwood, C. (1995) Benzoate-coenzyme A ligase, encoded by *badA*, is one of three ligases able to catalyze benzoyl-coenzyme A formation during anaerobic growth of *Rhodopseudomonas palustris* on benzoate, *J. Bacteriol. 177*, 6545−6551.
24. Caetano-Anolles, G. (1993) Amplifying DNA with arbitrary oligonucleotide primers, *PCR Methods Appl. 3*, 85−94.
25. O'Toole, G. A., and Kolter, R. (1998) Initiation of biofilm formation in *Pseudomonas fluorescens* WCS365 procceds via multiple, convergent signalling pathways: A genetic analysis, *Mol. Microbiol. 28*, 449−461.
26. Rutherford, K., Parkhill, J., Crook, J., Horsnell, T., Rice, P., Rajandream, M.-A., and Barrell, B. (2000) Artemis: Sequence visualization and annotation, *Bioinformatics 16*, 944−945.
27. Kovach, M. E., Elzer, P. H., Hill, D. S., Robertson, G. T., Farris, M. A., Roop, I., Martin, R., and Peterson, K. M. (1995) Four new derivatives of the broad-host-range cloning vector pBBR1MCS, carrying different antibiotic-resistance cassettes, *Gene 166*, 175−176.
28. Oda, Y., de Vries, Y. P., Forney, L. J., and Gottschal, J. C. (2001) Acquistion of the ability for *Rhodopseudomonas palustris* to degrade chlorinated benzoic acids as the sole carbon source, *FEMS Microbiol. Lett. 38*, 133−139.
29. Oda, Y., Wanders, W., Huisman, L. A., Meijer, W. G., Gottschal, J. C., and Forney, L. J. (2002) Genotypic and phenotypic diversity within species of purple nonsulfur bacteria isolated from aquatic sediments, *Appl. Environ. Microbiol. 68*, 3467−3477.
30. Oda, Y., Star, B., Huisman, L. A., Gottschal, J. C., and Forney, L. J. (2003) Biogeography of the purple nonsulfur bacterium *Rhodopseudomonas palustris*, *Appl. Environ. Microbiol. 69*, 5186−5191.
31. Oda, Y., Meijer, W. G., Gibson, J. L., Gottschal, J. C., and Forney, L. J. (2004) Analysis of diversity among 3-chlorbenzoate-degrading strains of *Rhodopseudomonas palustris*, *Microb. Ecol. 47*, 68−79.
32. van der Woude, B. J., de Boer, M., van der Put, N. M., van der Geld, F. M., Prins, R. A., and Gottschal, J. C. (1994) Anaerobic degradation of halogenated benzoic acids by photoheterotrophic bacteria, *FEMS Microbiol. Lett. 119*, 199−208.
33. Thompson, J. D., Higgins, D. G., and Gibson, J. T. (1994) CLUSTAL W: Improving the sensitivity of progressive multiple sequence alignment through sequence weighting, position-specific gap penalties and weight matrix choice, *Nucleic Acids Res. 22*, 4673−4680.
34. Bozdech, Z., Zhu, J., Joachimiak, M., Cohen, F., Pulliam, B., and DeRisi, J. (2003) Expression profiling of the schizont and trophozoite stages of *Plasmodium falciparum* with a long-oligonucleotide microarray, *Genome Biol. 4*, R9.
35. Rohlin, L., Trent, J. D., Salmon, K., Kim, U., Gunsalus, R. P., and Liao, J. C. (2005) Heat shock response of *Archaeoglobus fulgidus*, *J. Bacteriol. 187*, 6046−6057.
36. Ratushna, V., Weller, J., and Gibas, C. (2005) Secondary structure in the target as a confounding factor in synthetic oligomer microarray design, *BMC Genomics 6*, 31.
37. Hyduke, D. R., Rohlin, L., Kao, K. C., and Liao, J. C. (2003) A software package for cDNA microarray data normalization and assessing confidence intervals, *OMICS 7*, 227−234.
38. Tseng, G. C., Oh, M.-K., Rohlin, L., Liao, J. C., and Wong, W. H. (2001) Issues in cDNA microarray analysis: Quality filtering, channel normalization, models of variations and assessment of gene effects, *Nucleic Acids Res. 29*, 2549−2557.
39. Hartigan, N., Tharia, H. A., Sweeney, F., Lawless, A. M., and Papiz, M. Z. (2002) The 7.5-Å electron density and spectroscopic properties of a novel low-light B800 LH2 from *Rhodopseudomonas palustris*, *Biophys. J. 82*, 963−977.
40. Wellington, C. T., Taggart, A. K., and Beatty, J. T. (1991) Functional significance of overlapping transcripts of *crtEF*, *bchCA*, and *puf* photosynthesis gene operons in *Rhodobacter capsulatus*, *J. Bacteriol. 173*, 2954−2961.
41. Bauer, C. E., Buggy, J. J., Yang, Z. M., and Marrs, B. L. (1991) The superoperonal organization of genes for pigment biosynthesis and reaction center proteins is a conserved feature in *Rhodobacter capsulatus*: Analysis of overlapping *bchB* and *puhA* transcripts, *Mol. Gen. Genet. 228*, 433−444.
42. Ponnampalam, S. N., and Bauer, C. E. (1997) DNA binding characteristics of CrtJ. A redox-responding repressor of bacteriochlorophyll, carotenoid, and light harvesting-II gene expression in *Rhodobacter capsulatus*, *J. Biol. Chem. 272*, 18391−18396.
43. Simon, R., Priefer, U., and Pühler, A. (1983) A broad host range mobilization system for in vivo genetic engineering: Transposon mutagenesis in Gram negative bacteria, *Bio/Technology 1*, 784−790.
44. Zhulin, I. B., Taylor, B. L., and Dixon, R. (1997) PAS domain S-boxes in archaea, bacteria and sensors for oxygen and redox, *Trends Biochem. Sci. 22*, 331−333.

BI061074B